Biophysical Journal Volume 69 December 1995 2350–2363

Effects of pH Conditions on Ca^{2+} Transport Catalyzed by Ionophores A23187, 4-BrA23187, and Ionomycin Suggest Problems with Common Applications of These Compounds in Biological Systems

Warren L. Erdahl,* Clifford J. Chapman,* Richard W. Taylor,‡ and Douglas R. Pfeiffer*
*Department of Medical Biochemistry, The Ohio State University, Columbus Ohio 43210; and ‡Department of Chemistry and Biochemistry, University of Oklahoma, Norman, Oklahoma 73019 USA

ABSTRACT Phospholipid vesicles loaded with Quin-2 and 2′,7′-bis(2-carboxyethyl)-5(6)-carboxyfluorescein (BCECF) have been used to investigate the effects of pH conditions on Ca^{2+} transport catalyzed by ionophores A23187, 4-BrA23187, and ionomycin. At an external pH of 7.0, a ΔpH (inside basic) of 0.4–0.6 U decreases the rate of Ca^{2+} transport into the vesicles by severalfold under some conditions. The apparent extent of transport is also decreased. In contrast, raising the pH by 0.4–0.6 U in the absence of a ΔpH increases both of these parameters, although by smaller factors. The relatively large effects of a ΔpH on the transport properties of Ca^{2+} ionophores seem to reflect a partial equilibration of the transmembrane ionophore distribution with the H^+ concentration gradient across the vesicle membrane. This unequal distribution of ionophore can cause a very slow or incomplete ionophore-dependent equilibration of ΔpCa with ΔpH. A second factor of less certain origin retards full equilibration of ΔpCa when ΔpH = 0. These findings call into question several ionophore-based methods that are used to investigate the regulatory activities of Ca^{2+} and other divalent cations in biological systems. Notable among these are the null-point titration method for determining the concentration of free cations within cells and the use of ionophores plus external cation buffers to calibrate intracellular cation indicators. The present findings also indicate that the transport mode of Ca^{2+} ionophores is more strictly electroneutral than was thought, based upon previous studies.

INTRODUCTION

Use of the Ca^{2+} ionophores A23187, 4-BrA23187, and ionomycin to investigate cell signaling mechanisms sometimes involves tacit assumptions that are not fully supported by existing literature on the chemical and transport properties of these compounds. Important examples include the transport mode, which is usually assumed to be electroneutral. If this assumption were not valid, some actions of Ca^{2+} ionophores on cells could arise from ionophore-mediated membrane depolarization, with attendant effects on voltage-gated channels, rather than from a direct elevation of cytoplasmic Ca^{2+} concentration per se. As another example, when Ca^{2+} ionophores are used to calibrate fluorescent indicators trapped within cells or subcellular preparations, it is tacitly assumed that they rapidly and fully equilibrate transmembrane gradients of Ca^{2+} and H^+, or gradients of other cations. Were this assumption not valid, errors in estimates of intracellular cation concentrations could arise.

Model systems provide a means to test assumptions about the transport properties of Ca^{2+} ionophores without the many complications that arise when using cells or subcellular preparations. We recently utilized Quin-2-loaded vesicles prepared from 1-palmitoyl-2-oleoyl-*sn*-glycerophosphatidylcholine (POPC) for such purposes (Erdahl et al., 1994). During that work, models of the transport mechanism for these compounds (Pfeiffer et al., 1978; Taylor et al., 1982; Kauffman et al., 1983; Sankaram et al., 1987; Fasolato and Pozzan, 1989) were tested, particularly with respect to the possible existence of electrogenic modes (Chapman et al., 1987, 1990b; Fasolato and Pozzan, 1989; Stiles et al., 1991). In the absence of an imposed transmembrane potential, no electrogenic Ca^{2+} transport was observed, with a detection limit of ~1 in 10^4 events (Erdahl et al., 1994). That result is in accordance with earlier studies wherein Ca^{2+} transport catalyzed by A23187 was studied by using planar phospholipid bilayer techniques (Kafka and Holz, 1976; Wulf and Pohl, 1977; Moronne and Cohen, 1982). On the basis of these studies, it seems clear that the ionophores transport Ca^{2+} only by charge neutral mechanisms when there is no electrical potential across the membrane, or when there is a relatively small potential.

When a transmembrane potential of ~150 mv was imposed across the vesicle membrane, the initial rate of Ca^{2+} transport catalyzed by A23187 decreased by a few percent, whereas with ionomycin and 4-BrA23187 it increased by a few percent (Erdahl et al., 1994). Small effects of an imposed potential on the rate of ionophore-catalyzed Ca^{2+} transport have also been reported by Fasaloto and Pozzan (1989), who used both model membranes and cellular systems in their work. If it is assumed that these rate differences reflect the existence of electrogenic modes, then 1 in 10 events would be electrogenic when a large electrical potential is present. However, these small initial rate effects might also be caused by an influence of ΔpH on transport occurring via an exclusive electroneutral mode. This is because membrane H^+ permeability is potential-dependent (e.g., O'Shea et al., 1984), and uncatalyzed movements of

Received for publication 8 February and in final form 6 September 1995.

Address reprint requests to Douglas R. Pfeiffer, Ph.D., The Ohio State University, Department of Medical Biochemistry, 310A Hamilton Hall, 1645 Neil Avenue, Columbus, Ohio 43210-1218. Tel.: 614-292-5451; Fax: 614-292-4118; E-mail: pfeiffer.17@osu.edu.

0006-3495/95/12/2350/14 $2.00

H^+ (and/or other medium solutes) down its electrochemical gradient could progressively form a ΔpH (Erdahl et al., 1994). To further test the capacity of these ionophores to transport electrogenically, it is then necessary to understand how initial rates are influenced by ΔpH and by the absolute pH and to determine what magnitudes of ΔpH arise in the presence of an imposed potential.

Our previous study included several additional observations, which are difficult to explain without a better understanding of how transport catalyzed by Ca^{2+} ionophores is affected by ΔpH and by absolute pH. For example, it was shown that these ionophores do not readily equilibrate Ca^{2+} with a high affinity chelator (Quin-2) when these agents are separated by a membrane, that apparent extents of transport show a complex dependence on ionophore concentration, and that the kinetics of transport and the dependence of these on Ca^{2+} concentration show multiphasic features. (Erdahl et al., 1994). In the present report we describe the use of POPC vesicles loaded with the fluorescent pH indicator 2′,7′-bis-(2-carboxyethyl)-5(6)-carboxyfluorescein (BCECF) (Rink et al., 1982) together with the Ca^{2+} indicator/chelator Quin-2 (Tsien, 1980) to investigate the role of pH conditions in establishing the transport properties of Ca^{2+} ionophores. The results strengthen the case against electrogenic transport modes for these commonly used Ca^{2+} ionophores, but indicate that caution is warranted when an application requires full equilibration of transmembrane cation gradients.

MATERIALS AND METHODS

Reagents

Synthetic POPC was obtained from Avanti Polar Lipids (Alabaster, AL) and used as provided. A23187, ionomycin, valinomycin, and nigericin were obtained from Calbiochem (LaJolla, CA). 4-BrA23187 was obtained from Sigma (St. Louis, MO). Ionophore stock solutions were prepared in ethanol. Stock solutions of Ca^{2+} ionophores were standardized as described previously (Erdahl et al., 1994). Valinomycin and nigericin solutions were prepared by weight. Quin-2 (K^+ salt) and BCECF (free acid) were obtained from Sigma and Molecular Probes (Eugene, OR), respectively. Quin-2 was purified and converted to the Cs^+ or the K^+ form on Chelex 100 columns (Erdahl et al., 1994).

Preparation of phospholipid vesicles

Quin-2-loaded POPC vesicles were prepared by the freeze-thaw-extrusion technique (Hope et al., 1985; Mayer et al., 1986) as previously described (Erdahl et al., 1994), using polycarbonate membrane filters with a 100-nm pore size. Normally, the vesicles also contained BCECF, which was present in the formation media at 80 μM. These media were buffered with 10 mM Hepes, and the pH was adjusted to 7.0 by the addition of ultrapure CsOH, KOH, or the acid form of Hepes, as required. After vesicle formation, external dyes were removed by passing the preparations over Sephadex G-50 minicolumns (Fry et al., 1978). The columns were eluted by low-speed centrifugation (Fry et al., 1978) and had been equilibrated previously with 10 mM Hepes, pH 7.0, with the counter ion (Cs+ or K^+) being the same as that trapped inside. The amount of Quin-2 entrapped was determined by spectral titrations with a standard $CaCl_2$ solution after dispersion of the vesicles with deoxycholate (Erdahl et al., 1994). Trapped cations were determined by atomic absorption measurements after dispersion of the vesicles with 0.1 N HCl (Chapman et al., 1991). (The samples used to determine trapped cations had been passed over Sephadex columns equilibrated with Na^+ Hepes to avoid the presence of external Cs^+ or K^+ when measuring the internal content of these cations.) The nominal POPC concentration in vesicle suspensions was determined by measurement of lipid phosphorous (Bartlett, 1959). The concentrations of entrapped solutes were then calculated using these analytical data and an internal volume of 3.03 μl/ml for a nominal POPC concentration of 1.5 mM (Chapman et al., 1990a).

Estimation of intravesicular buffer concentration and ionic strength

The concentrations of solutes entrapped in vesicles formed by freeze-thaw extrusion do not approximate those in the vesicle-forming medium because of a freeze-related concentrating effect, which is seen to a variable degree depending on the solute in question and its concentration (Chapman et al., 1990a, 1991). Accordingly, buffer entrapment and internal ionic strength were also calculated from measured parameters on the basis of the following. The acid form of Hepes is zwitterionic within the pH range at which it is useful as a buffer (pK_a = 7.55) (Vega and Bates, 1976). When a fraction of Hepes is ionized by addition of a strong base to form a buffer, the basic form that is generated is anionic, and the solution concentration of this form is equal to that of the strong base counter ion (in this case Cs^+ or K^+), which was used to adjust the pH. Thus, when vesicles are formed in a medium containing only Hepes buffer, the internal buffer concentration can be calculated from the internal $Cs^+(K^+)$ concentration and the internal pH by use of the Henderson-Hasselbach equation. When the vesicles contain Hepes and Quin-2, the internal $Cs^+(K^+)$ concentration is equal to the internal Hepes anion concentration plus an additional component that is present as the counter ion to Quin-2. Because pK_a values for the Quin-2 ionizable carboxylic acid functions are known (e.g., Yuchi et al., 1993), the ionization state of Quin-2 at pH values of interest can also be calculated. We used a value of 3.9 for this parameter because Quin-2 approaches full ionization at pH 7 and above. The measured internal Quin-2 concentration is then multiplied by 3.9 and the result subtracted from the total internal $Cs^+(K^+)$ concentration to yield the concentration of $Cs^+(K^+)$, which is referable to entrapped Hepes anion. The internal buffer concentration was then calculated as described for vesicles that did not contain Quin-2. For the vesicles used here, this method would give an internal Hepes concentration of 63.5 ± 14.7 mM (n = 10) if the internal pH was assumed to be the same as that of the formation medium (7.0), and the internal volume was taken to be 3.03 μl/ml at a 1.5 mM concentration of POPC (Chapman et al., 1990a). However, the observed internal pH was ~7.4 even though the formation medium was at pH 7.0 (see Results). We used the observed value of internal pH, which gave an internal Hepes concentration of 33.7 ± 7.6 mM.

Regarding the estimation of internal ionic strength (initial values), we assumed that the anionic moieties of Quin-2 contribute as independent charges (Smith and Miller, 1985). In that case, the internal ionic strength is simply the internal concentration of $Cs^+(K^+)$ because there are no other cations present in these vesicles and the zwitterionic form of Hepes will not contribute to the value (Fabiato and Fabiato, 1979). By this method, the internal ionic strength was estimated to be 60 ± 5 mM (n = 10). Table 1 summarizes the internal solute concentrations in these vesicles and some related parameters.

Determination of Ca^{2+} transport, intravesicular pH, and membrane potential

All data were obtained at 25°C. Ca^{2+} transport was initiated by the manual addition of ionophores and was followed by monitoring formation of the Ca^{2+}:Quin-2 complex, which was in turn monitored by difference absorbance measurements carried out with an Aminco DW2a dual wavelength spectrophotometer. The wavelengths used were 264 vs. 338 nm. Some reagents added during these experiments produced small absorbance dif-

TABLE 1 POPC vesicle properties and solute contents

Parameter	Value
*Average diameter	70 nm
Entrapped volume (at 1.5 mM POPC)	3.03 μl/ml
*Internal Quin-2 concentration	10.5 ± 0.8 mM (n = 10)
Internal BCECF concentration	N.D.
*Internal Cs^+ (K^+) concentration	60 ± 5 mM (n = 10)
Internal Hepes concentration	33.7 ± 7.6 mM (n = 10)
*Internal pH (observed)	7.3 – 7.5
Internal ionic strength	60 ± 5 mM (n = 10)
Predicted internal osmotic pressure	~110 mOsM

Values were obtained as described in Materials and Methods or as shown in Chapman et al. (1990).
*These parameters were measured quantities, whereas the others were calculated.

ferences at this wavelength pair because of their own spectral characteristics. These were accounted for by editing the data files before further analysis. Appropriate segments of the progress curves were fit to Eq. 1 and to Eq. 2 or 3 to extract the initial rate and the projected extents of transport, respectively, as described previously (Erdahl et al., 1994).

$$A_T = A_o + Bt + Ct^2 \quad (1)$$

$$A = A_m^2 kt/(1 + A_m kt) \quad (2)$$

$$A = A_{m1}(1 - e^{-k_1 t}) + A_{m2}(1 - e^{-k_2 t}). \quad (3)$$

In Eq. 1, A_T and A_o are the observed and initial absorbance values, respectively, B is the initial rate, C is a correction factor for nonlinearity, and t is time. In Eq. 2, A represents the Ca^{2+} transported at time t expressed in units of μM external concentration, A_m is maximal Ca^{2+} transport, and k is the rate constant. The designations in Eq. 3 are analogous to those in Eq. 2, with A_{m1}, A_{m2}, k_1, and k_2 referring to the characteristics of the early and later segments of the progress curves, respectively. Absorbance values and Ca^{2+} concentrations were interrelated by referring to a standard curve, which was obtained by titrating deoxycholate-lysed, Quin-2-containing vesicles with standard $CaCl_2$ (Erdahl et al., 1994).

The intravesicular pH was estimated from the fluorescence signal of entrapped BCECF with emission determined at 535 nm. The ratio of emission intensities observed when the excitation wavelength was at an isofluoresence point versus the maximum in the excitation spectrum indicates the protonation state of the dye (Rink et al., 1982). An SLM 8000 DS photon-counting fluorometer equipped with dual grating monochromators was used for these measurements, and the response of the dye to internal pH was calibrated by a method presented in the Results section. The fluorometer was operated in A/B mode so that measurements of fluorescence intensity were corrected for variations in source intensity as a function of wavelength. With this instrument, the repetitive scan rate is relatively slow, limiting the usefulness of this approach to obtaining excitation ratios as a function of time. Accordingly, ratios were obtained in some of the experiments by performing duplicate incubations in which one or the other excitation wavelength was used to monitor the state of BCECF. The ratios were then calculated at each sampling time using a computer that was interfaced to the fluorometer and also used for data collection. Initial comparison experiments, conducted under conditions in which the transport rate was slow, showed no differences in ratio data obtained by this method compared with the repetitive scanning method.

Measurements of membrane potential (inside negative) across the vesicle membrane were made with a tetraphenylphosphonium (TPP^+) electrode (Kamo et al., 1979). The medium contained 3.33 μM TPP·Cl when these experiments were conducted.

RESULTS

Spectral and pK_a properties of BCECF in phospholipid vesicles

To allow determination of intravesicular pH together with Ca^{2+} transport, vesicles loaded with BCECF together with Quin-2 were prepared by established methods (Hope et al., 1985; Mayer et al., 1986; Chapman et al., 1990a, 1991). BCECF is efficiently entrapped during vesicle preparation, as judged qualitatively by fluorescence intensity, to an extent that is influenced by medium pH. The entrapment was independent of pH over the range of 8.5 to ~7, but it increased at lower values. At pH 5, the lowest value investigated, the amount of BCECF entrapped was approximately twice that seen above pH 7 (data not shown).

Figs. 1 and 2 compare fluorescence spectral properties and pK_a properties of BCECF in homogeneous solution with those seen when the indicator is entrapped in POPC vesicles. In solution (Fig. 1), the excitation spectra obtained across a pH range of ~5–10 show an isofluorescence point near 438 nm, with the anionic form fluorescing maximally when excited near 503 nm (Fig. 1 *A*). The ratio of emission intensities (R) observed when the excitation wavelength was 503 nm vs. 438 nm was fit as a function of pH to Eq. 4 to obtain pK_a and the minimum (R_{min}) and maximum (R_{max}) values of the emission ratio parameter.

$$R = \frac{R_{min} + R_{max} 10^{(pH - pK_a)}}{10^{(pH - pK_a)} + 1}. \quad (4)$$

Fig. 1 *B* shows that data obtained from *A* are well represented by Eq. 4, which yielded a pK_a value of 7.06 and minimum and maximum values for the emission ratio parameter of 0.60 and 13.8, respectively. The effect of KCl concentration (ionic strength) on these parameters is shown in Fig. 1 *C*. The observed value of pK_a decreased from ~7.6 to ~7.0 as the KCl concentration was increased from 0 to 200 mM. The minimum and maximum values of the ratio parameter were not significantly affected, however.

The data shown in Fig. 1 *C* emphasize that ionic strength must be taken into account when assigning a pK_a value to entrapped BCECF, if reasonably accurate values of absolute internal pH are to be obtained. As described in Materials and Methods, the ionic strength in vesicles prepared in media containing only Hepes and Quin-2 will be equal to the concentration of the monovalent cation (Cs^+ or K^+), if it is assumed that the internal salts are fully dissociated and that the anionic moieties of Quin-2 contribute independently. Taking the entrapped volume at 1.5 mM POPC (nominal) to be 3.03 μl/ml (Chapman et al., 1990a) and using the observed values of Cs^+ or K^+ entrapment (Table 1), the internal ionic strength in these vesicles was estimated to be 60 ± 5 mM (n = 10). When this value is compared with the solution data shown in Fig. 1 *C*, it is seen that a pK_a value of ~7.2 is expected for BCECF entrapped within the vesicles used for this study.

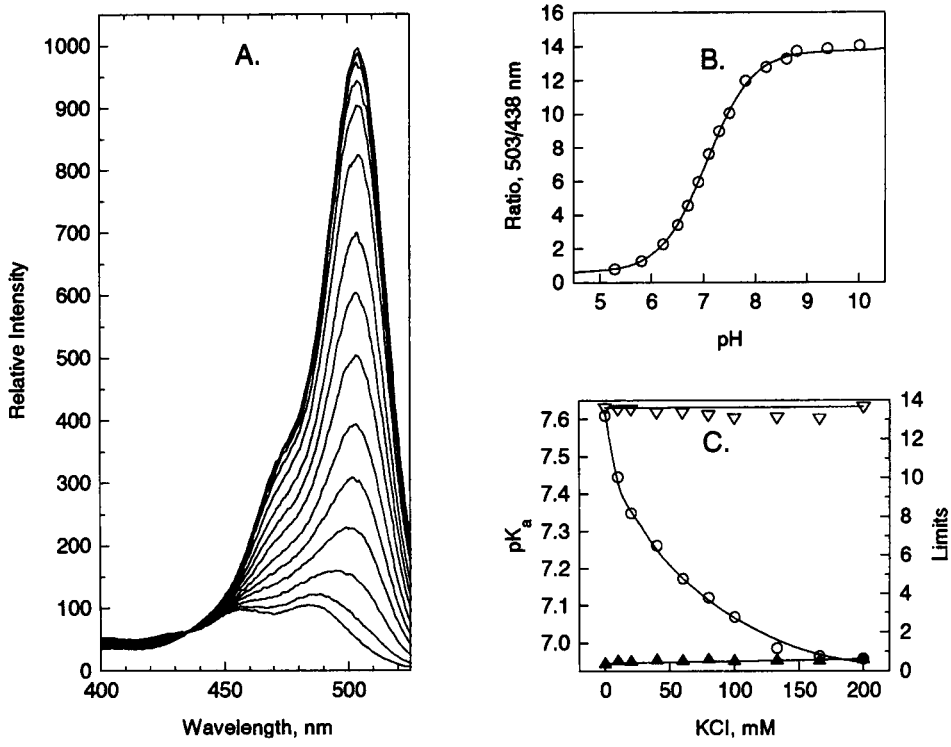

FIGURE 1 Spectral and pK_a properties of BCECF in homogeneous solution. Data were obtained at 25°C using water solutions containing 3 mM Hepes (K^+), various concentrations of KCl, and BCECF at 0.5 μM. (*A*) Excitation spectra of BCECF (emission wavelength = 535 nm) over the pH range of ~5.2 (bottom spectrum) to ~10.1 (top spectrum). The KCl concentration was 100 mM. Data have been corrected for variations in the source emission intensity as a function of wavelength. (*B*) Intensity ratios with excitation at 503 vs. 438 nm were calculated from each spectrum shown in A and plotted as a function of pH. These values were fit to Eq. 4 (see Results) by a nonlinear least-square technique, with the solid line showing the best fit obtained. (*C*) pK_a (○) plus the minimum (▲) and maximum (Δ) values of the intensity ratio parameter are shown as a function of the KCl concentration in the medium. Each set of values was obtained from an experiment like the one illustrated in A and B.

Excitation spectra of BCECF entrapped in vesicles are shown in Fig. 2. In Fig. 2 *A*, the Quin-2 that was also entrapped was free, whereas in Fig. 2 *B* it was largely saturated with Ca^{2+}. In these experiments, valinomycin plus carbonyl cyanide *p*-chlorophenylhydrazone (CCP) was present to promote equilibration between internal and external pH. The external pH was then varied over the same range used for the homogeneous solution studies to yield a number of internal pH values within this range. Considering first the spectra per se, it is seen that the isofluorescence wavelength is poorly defined or absent, with all spectra tending toward a common baseline in the shorter wavelength region. We attribute the absence of a well-defined isofluorescence wavelength to the light scattering properties of the vesicle suspensions. A light scattering trace, in arbitrary units, is superimposed upon the excitation spectra shown in Fig. 2 *B*. It shows that the extent of light scattering increases markedly with decreasing wavelength, as expected for suspensions of these vesicles, which have a diameter of ~70 nm (Chapman et al., 1990a). The effective excitation source intensity will vary as an inverse function of scattering. Accordingly, the small fluorescence yield of the BCECF acid form should be suppressed progressively at shorter lengths, and this factor may be responsible for the poorly defined isofluorescence point.

The considerations mentioned above raise the question of what value to use for the isofluorescence wavelength of BCECF entrapped in vesicles. The isofluorescence wavelength is related to the absorption spectrum of BCECF, and the absorption spectrum is not likely to be altered by entrapment. Accordingly, we used the isofluorescence wavelength observed in solution (438 nm), even though it does not seem to be a strict isofluorescence point within these sets of spectra. When this is done, and 503 nm is again taken as the excitation wavelength producing maximal fluorescence of the anionic form, the emission intensity ratio as a function of pH is again well represented by Eq. 4, regardless of whether the entrapped Quin-2 is free or complexed with Ca^{2+} (Fig. 2, *C* and *D*). The observed value of pK_a (7.31) is close to that expected from the solution study (Fig. 1) and the estimate of intravesicular ionic strength, as are the minimum and maximum values of the ratio parameter (Table 2). No significant variations in these parameters are seen when internal and external pH are equilibrated with valinomycin plus CCP, valinomycin plus nigericin, or valinomycin plus nigericin and CCP (Table 2).

To further test the reliability of these measurements, the pK_a of entrapped BCECF was determined using vesicles prepared in the absence of Quin-2 and in medium containing a low buffer concentration (3 mM) so as to minimize internal ionic strength. The value obtained under those conditions was 7.67 (data not shown), again close to what is expected on the basis of the solution data shown in Fig. 1 *C*. Thus, there is no indication that BCECF is differently effected by ionic strength when confined to the vesicle lumen. Finally, the consequences of mismatching the initial internal and external K^+ concentrations during calibration experiments on the apparent value of pK_a were also investigated. Assuming that valinomycin plus CCP or valinomycin plus nigericin fully equilibrate the transmembrane concentration gradients of K^+ and H^+, the following relationship is ap-

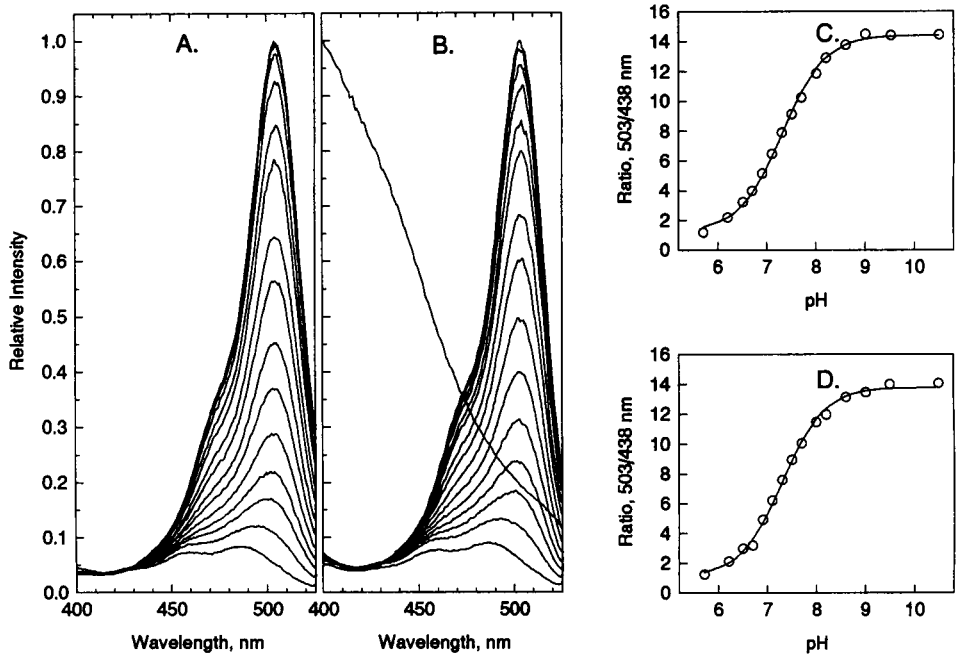

FIGURE 2 Spectral and pK_a properties of BCECF in POPC vesicles. Data were obtained at 25°C using suspensions of POPC vesicles that contained entrapped BCECF plus Quin-2 and were prepared as described in Materials and Methods. The nominal concentrations of POPC and entrapped Quin-2 were 1.5 mM and 29 μM, respectively. The internal ionic strength (K^+ concentration) was 60 ± 5 mM (n = 10), estimated as described in Materials and Methods. The vesicles were initially suspended in 60 mM KCl and 10 mM Hepes (K^+), pH 7.00. The medium also contained 5.0 μM CCP plus 0.5 μM valinomycin to promote equilibration of internal and external pH. (*A*) There were no further additions except for KOH or the acid form of Hepes, which were used to adjust the pH. BCECF excitation spectra were recorded over an external pH range of ~5.7 (bottom spectrum) to ~10.7 (top spectrum), with emission monitored at 535 nm. (*B*) Analogous conditions were used, except that the medium also contained 1 mM $CaCl_2$ plus 1 μM ionomycin to convert internal Quin-2 to the Quin-2:Ca^{2+} complex. (*C* and *D*) Intensity ratios with excitation at 503 vs. 438 nm, calculated from each spectrum shown in A and B, respectively, and plotted as a function of external pH. These values were fit to Eq. 4 (see Results) by a nonlinear least-squares technique, with the solid line showing the best fit obtained. In addition to the above, B shows a light-scattering spectrum superimposed upon the excitation spectra. The scattering spectrum was obtained at pH ~7 by locking the excitation and emission monochromators together and scanning them across the wavelength range shown. Other medium and instrumental conditions were the same as those used to obtain the excitation spectra.

plicable for each point obtained during calibration (Thomas et al., 1979).

$$\frac{(K^+)_{out}}{(K^+)_{in}} = \frac{(H^+)_{out}}{(H^+)_{in}}. \quad (5)$$

Both the internal and external K^+ concentrations must change as pH is adjusted during calibration to a degree that is dependent on several interactive factors (initial internal and external K^+ concentrations, buffer concentrations, volume, and ionic strength changes associated with maintenance of osmotic pressure equilibrium, and others). Accordingly, a dependence of the apparent pK_a value of entrapped BCECF on the external K^+ concentration that is present during calibration is expected. This dependence is shown experimentally in Fig. 3, where it is seen that each log unit change in the initial external K^+ concentration produces a change of −0.65 in the apparent pK_a value of the indicator.

TABLE 2 The pK_a and maximal and minimal excitation ratio properties of BCECF in Quin-2-loaded POPC vesicles

Condition	pK_a	R_{max}	R_{min}
Free Quin-2			
Valinomycin + CCP	7.31	13.9	1.12
Valinomycin + nigericin	7.31	13.6	1.09
Valinomycin + CCP and nigericin	7.32	13.9	1.12
Ca^{2+}:Quin-2			
Valinomycin + CCP	7.31	14.1	1.09
Valinomycin + nigericin	7.29	13.5	1.12
Valinomycin + CCP and nigericin	7.31	14.3	1.15

Values were obtained as described in Materials and Methods and the legend to Fig. 2.

Thus there is a small uncertainty (about 0.1 log units) in the pK_a value of entrapped BCECF because there is incomplete agreement between the external and internal calibration methods. The external method might not be fully reliable because entrapment might produce subtle changes in the properties of the indicators. The internal method is subject to small errors related to estimation of the internal K^+ concentration and related factors. For this work, we have split the difference between the two methods, taking the pK_a of entrapped BCECF to be 7.25 at an ionic strength of 60 mM. The maximum and minimum values of the emission ratio parameter were taken to be 13.9 and 1.10, respectively, which are the means of all values shown in Table 2. As will be shown below, the uncertainties in these values are sufficiently small for our present purposes.

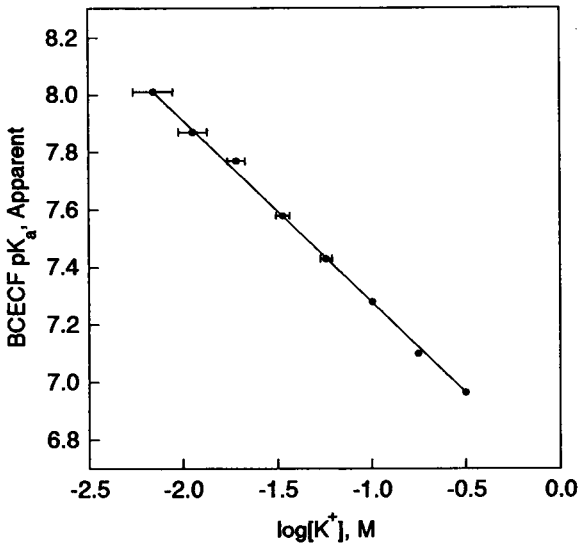

FIGURE 3 Apparent pK_a of entrapped BCECF as a function of the external K^+ concentration. Values were obtained as described for Fig. 2, *A* and *C*, except that the external Hepes concentration was 3 mM and the initial external KCl concentration was varied from 6 mM to 316 mM, as shown. External pH was adjusted by the addition of KOH, which significantly altered the initial external K^+ concentration in the lower region of the range investigated. The range of variation is illustrated, when it was significant, by plotting the *x* axis value as a bar instead of a point.

Rates and extents of Ca^{2+} uptake as a function of pH conditions

In our earlier report we showed that A23187 seems to not fully equilibrate Ca^{2+} with Quin-2 when the two reagents are separated by a POPC vesicle membrane (Erdahl et al., 1994). In the case of Ca^{2+} transport into Quin-2-loaded vesicles, two potential explanations were suggested. In one it was considered possible that internal pH reaches a high value, such that the availability of protonated ionophore at the inner membrane interface becomes low enough to severely limit the overall rate of the forward reaction (Ca^{2+} uptake). In the other, rising internal pH and a consequent redistribution of ionophore between the two membrane surfaces was seen as progressively favoring the reverse reaction (Ca^{2+} release), thereby limiting the net rate of Ca^{2+} uptake in spite of the excess of free Quin-2 within the vesicle interior. Fig. 4 examines relationships between the rate and extent of Ca^{2+} uptake and intravesicular pH under conditions in which total Ca^{2+} is in approximately fourfold excess of entrapped Quin-2 and transport is catalyzed by A23187. In all three panels, it is seen that the internal pH, as indicated by BCECF, is 0.3–0.4 U higher than the pH at which the vesicles were formed, and thus a ΔpH of this magnitude exists at the beginning of the experiments. (The presence of an inside basic ΔpH in vesicles formed by freeze-thaw extrusion is probably caused by a more efficient entrapment of Hepes base compared with the acidic form of Hepes. That entrapment efficiency can vary with the ionization state of an acidic compound is shown by the effect

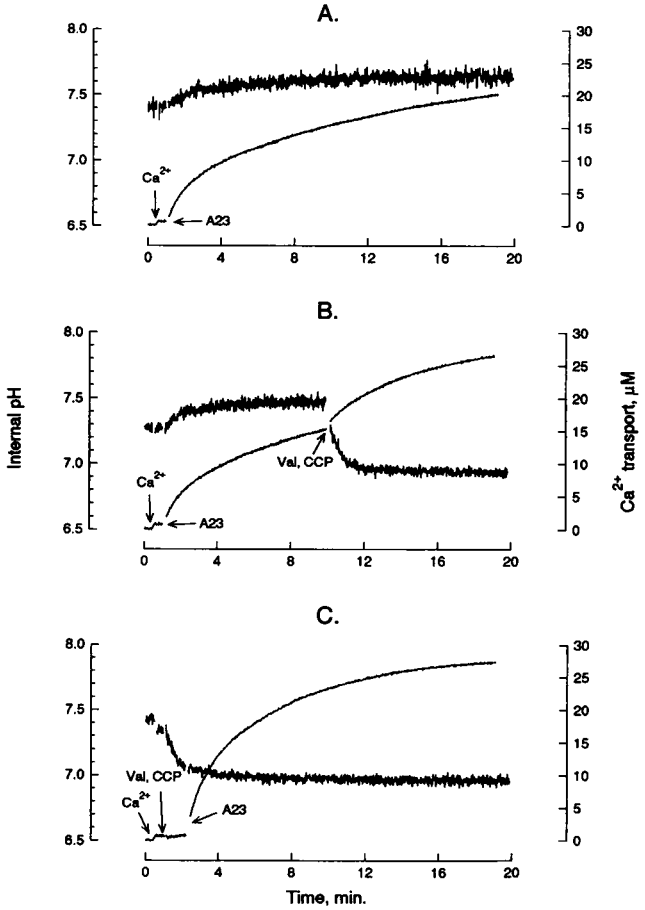

FIGURE 4 Relationships between Ca^{2+} transport by A23187 and intravesicular pH. POPC vesicles were incubated as described in the legend to Fig. 2, except that the nominal concentration of entrapped Quin 2 was 28 μM. Data displaying lower and higher degrees of scatter correspond to Ca^{2+} transport and intravesicular pH, respectively, which were monitored as described in Materials and Methods and the legend to Fig. 2. $CaCl_2$ (100 μM), A23187 (0.2 μM), valinomycin (0.5 μM), and CCP (5.0 μM) were added as indicated in the three panels.

of pH on BCECF entrapment described in the first paragraph of the Results section.) The addition of A23187 to initiate Ca^{2+} uptake under these conditions produces a progress curve that shows little or no initial linear segment in spite of the high affinity of Quin-2 for Ca^{2+} and the presence of excess Ca^{2+} (Fig. 4 *A*). A visual examination of the overall progress curve also suggests that net uptake of Ca^{2+} is approaching a maximum value, which is less than the amount of entrapped Quin-2. As was shown previously, progress curves of these types are best represented by the expression for a biexponential decay (Eq. 3, Materials and Methods), and fitting the data in Fig. 4 *A* to to this expression yields 88% of the available Quin-2 as the projected maximal extent of transport (Table 3). The unexpected features of this progress curve (the absence of a linear segment and the limited extent) are not caused by exceeding the internal H^+ buffering capacity because the internal pH increases by only 0.2–0.3 U over the full time course of the experiment to yield a final value near 7.6 (Fig. 4 *A*). This

TABLE 3 Effects of ΔpH on rates and extents of Ca^{2+} transport

Conditions	A23187	4-BrA23187	Ionomycin
Panels A			
Initial rate	0.130	0.143	0.087
Extent	88.0	83.8	86.8
Panels B			
Rate before Valinomycin + CCP	0.012	0.014	0.014
Rate after Valinomycin + CCP	0.108	0.051	0.043
Extent	100.2	91.9	97.6
Panels C			
Initial rate	0.200	0.249	0.136
Extent	99.6	91.0	95.4

Rate values are given in units of μM/sec, whereas the extent values are given as the percentage of total Quin-2. These values are from the experiments shown in Figs. 4–6 and were obtained by fitting appropriate portions of the progress curves to Eqs. 1 and 3 as described previously (Erdahl et al., 1994).

value of internal pH could not greatly limit the availability of protonated A23187 at the inner membrane interface, and hence the forward rate of Ca^{2+} transport, because the pK_a of A23187 associated with phosphatidylcholine bilayers is 7.85 (Kaufmann et al., 1982).

Nevertheless, the slightly basic internal pH is an important factor in producing the unexpected features as shown in Fig. 4, *B* and *C*. Fig. 4 *B* shows that the addition of valinomycin plus CCP during Ca^{2+} uptake reduces the internal pH to 7.0, the same value that exists in the external medium. This collapse of ΔpH accelerates Ca^{2+} uptake by approximately ninefold compared with the immediately preceding rate, and it allows the uptake reaction to proceed sufficiently to saturate the internal Quin-2 (Table 3). If ΔpH is collapsed before initiating Ca^{2+} uptake (Fig. 4 *C*), the internal pH remains near 7.0 throughout the subsequent period of Ca^{2+} accumulation. Under these conditions, an approximately linear initial segment is seen and the extent of uptake proceeds to saturation of internal Quin-2 (Table 3). Progress curves of this type are well represented by the expression for a second-order decay (Eq. 2, Materials and Methods) as well as a biexponential decay (Eq. 3) (data not shown). Fitting the data in Fig. 4 *C* to Eq. 1 gave an initial rate of Ca^{2+} uptake, which is 1.6 times larger than the value obtained under the conditions of Fig. 4, *A* and *B* (Table 3).

The marked effects of a small ΔpH on the rates and extents of Ca^{2+} transport are not limited to transport catalyzed by A23187. Behavior very similar to that shown in Fig. 4 was observed with 4-BrA23187 and with ionomycin (Figs. 5 and 6, Table 3). Similar behavior was also observed for all three ionophores when ΔpH was collapsed by the use of nigericin instead of valinomycin plus CCP, whereas neither valinomycin nor CCP used alone had much effect on ΔpH or on Ca^{2+} transport (data not shown).

In contrast to the inhibition of Ca^{2+} influx that is associated with a small increase in internal versus external pH, raising the pH in the absence of a ΔpH accelerates forward Ca^{2+} transport (A23187 and ionomycin) or has essentially

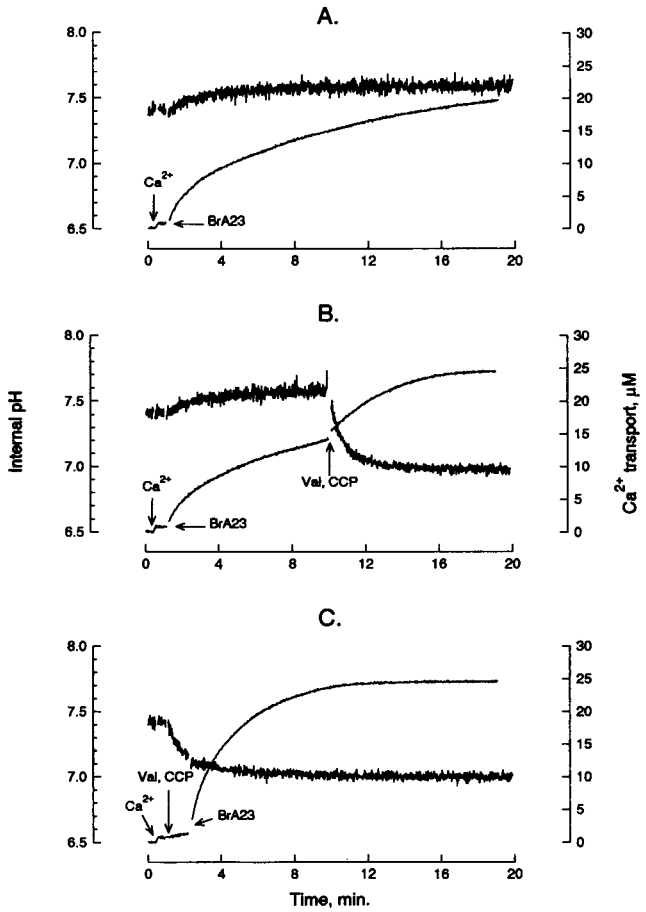

FIGURE 5 Relationships between Ca^{2+} transport by 4-BrA23187 and intravesicular pH. Conditions were the same as described in the legend to Fig. 4 except that 6.0 μM 4-BrA23187 was used in place of A23187.

no effect (4-BrA23187). This is shown in Fig. 7 *A* in which the initial rates of the forward reaction are given as a function of medium pH values ranging from 6 to 9. These data were obtained in the presence of valinomycin plus CCP, and so the pH values given will pertain in both internal and external volumes (Fig. 2). Fig. 7 *B* shows the extents of transport under the same conditions as those employed in *A*. When ΔpH is absent, the forward reaction proceeds (essentially) to completion in all cases except pH 6 and 6.5, where a significant competition is expected between the Ca^{2+} and H^+ for association with Quin-2 and the Ca^{2+} ionophores.

Poor equilibration between ΔpCa and ΔpH under conditions similar to those employed when using ionophores in biological systems

Because insufficient internal buffering cannot explain the unexpected features of the Ca^{2+} ionophore transport curves, the second potential explanation noted above may be playing a role (i.e., ionophore redistribution in accordance with ΔpH). It is important to determine whether this occurs because some of the purposes for which Ca^{2+} ionophores are used in cell biology involve the tacit assumption that

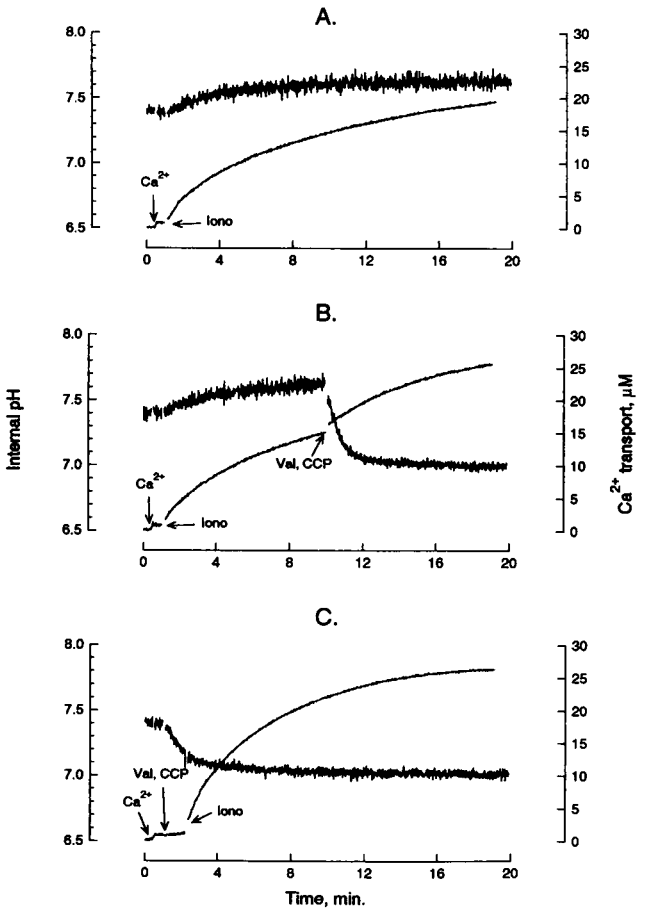

FIGURE 6 Relationships between Ca^{2+} transport by ionomycin and intravesicular pH. Conditions were the same as described in the legend to Fig. 4 except that 0.3 μM ionomycin was used in place of A23187.

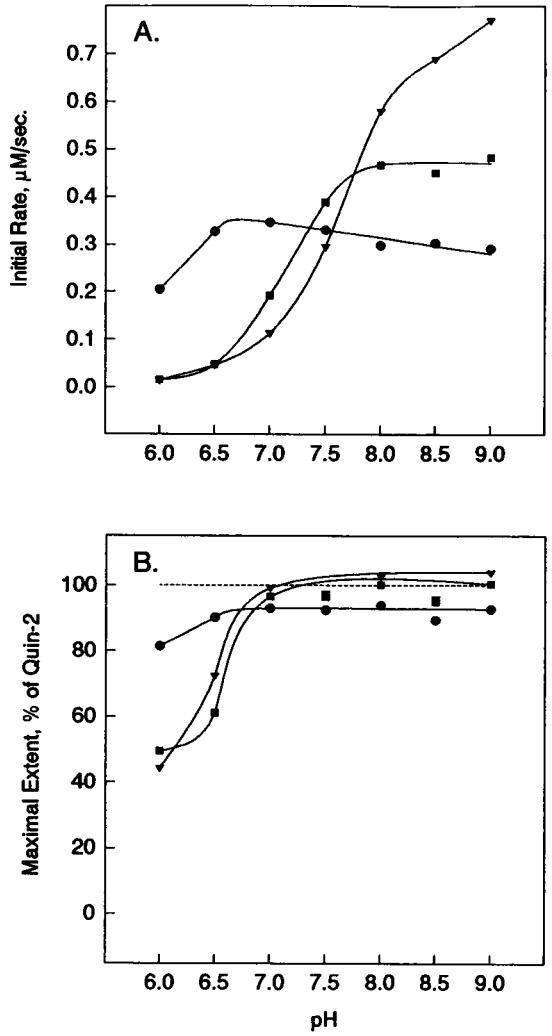

FIGURE 7 The effect of pH on ionophore-catalyzed cation transport in the absence of a ΔpH. Data were obtained from experiments like those shown in Figs. 4 *C*, 5 *C*, and 6 *C*, in which valinomycin and CCP were added before the Ca^{2+} ionophore to maintain internal pH at the external value that was varied as shown. Data were fit to Eq. 1 to obtain the initial rates of transport (*A*) and to Eq. 3 to obtain the projected extents of transport (*B*), respectively. An extent value of 100% corresponds to the nominal concentration of entrapped Quin-2, which in this experiment was 33 μM. For both panels the Ca^{2+} ionophore conditions were as follows: (■), 0.2 μM A23187; (●), 6.0 μM 4-BrA23187; (▼), 0.3 μM ionomycin.

they readily equilibrate transmembrane Ca^{2+} gradients or equilibrate these gradients with pH gradients, and an unequal distribution of ionophore could limit the rate at which these equilibrations are attained (see Discussion). Extents of equilibration can be investigated with the present model system as illustrated in Figs. 8 and 9. When obtaining the data shown in Figs. 8 and 9, the conditions of pH, free Ca^{2+} concentration, and ionophore concentration were adjusted to mimic those that often exist when the compounds are applied to intact cells or subcellular structures. In both figures, a low concentration of ionophore was used to load the vesicles with Ca^{2+}, to a point at which the internal Quin-2 was approaching saturation. EDTA was then added to the external medium, and Ca^{2+} efflux from the vesicles was observed. These experiments were performed with each of the three ionophores in the absence (Fig. 8) or presence (Fig. 9) of a ΔpH. In all cases it is seen that projected extents of Ca^{2+} efflux are a function of the ionophore concentration, which was present after the addition of EDTA. This concentration dependence would not be observed if the ionophores equilibrated ΔpH with ΔpCa in a straightforward manner. Instead, a constant extent of release with only the rate varying with ionophore concentration would be seen.

Figs. 8 and 9 also show that there are marked differences between the three ionophores with respect to the extents of release that occur at a given concentration and with respect to how release is influenced by a ΔpH. These differences are considered below in a more quantitative fashion.

DISCUSSION

Use of BCECF in vesicle systems

The present results show that BCECF can be used in Quin-2-loaded vesicles to investigate the relationships between

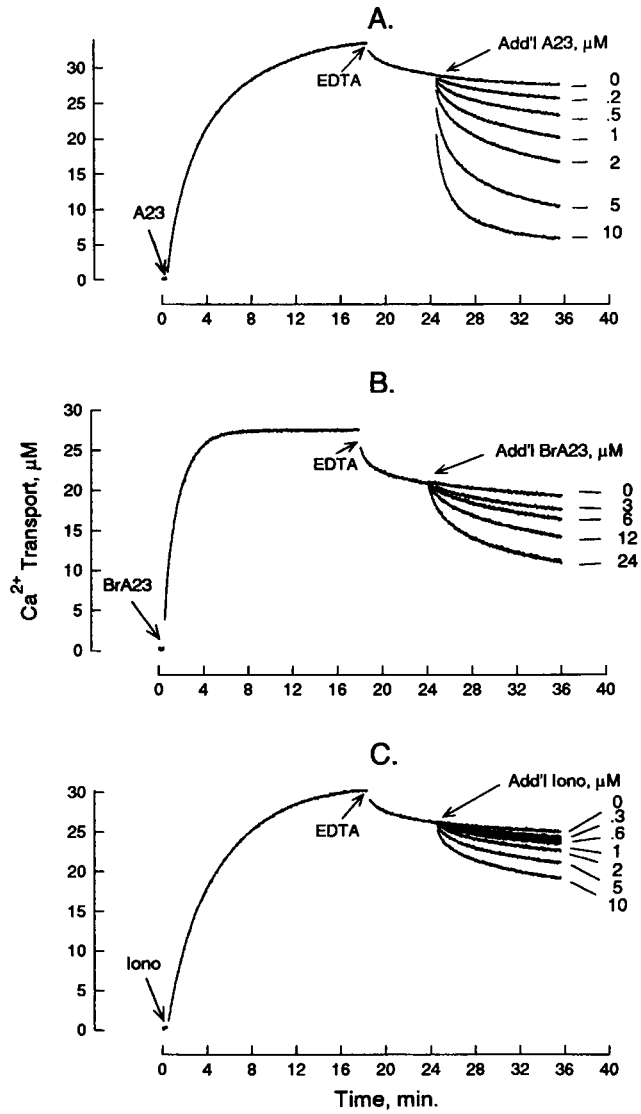

FIGURE 8 The effect of ionophore concentration on the EDTA-dependent release of Ca^{2+} from Quin-2:Ca^{2+}-loaded vesicles in the absence of a ΔpH. Vesicles containing Quin-2 and BCECF were initially loaded with Ca^{2+} by the addition of 0.2 μM A23187 (*A*), 6.0 μM 4-BrA23187 (*B*), or 0.3 μM ionomycin (*C*). The medium concentration of $CaCl_2$ was 100 μM, and valinomycin (0.5 μM) plus CCP (5.0 μM) were present initially in all cases. As Ca^{2+} transport into the vesicles approached a limiting value, 1.00 mM EDTA (pH 7.0) was added, and the resultant Ca^{2+} efflux was observed. Five minutes later, additional ionophore was added at the concentrations shown on the right side of the individual panels, and observation of Ca^{2+} efflux was continued. Parallel experiments were conducted in the fluorometer to monitor intravesicular pH throughout, although these data are not shown in the figure.

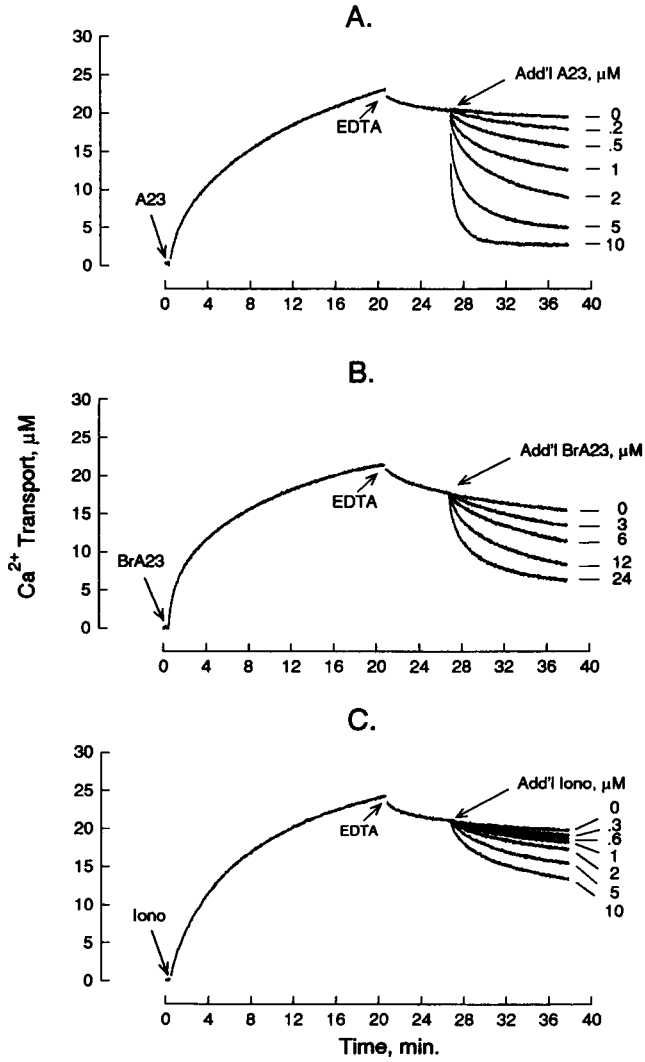

FIGURE 9 The effect of ionophore concentration on the EDTA-dependent release of Ca^{2+} from Quin-2:Ca^{2+}-loaded vesicles in the presence of a ΔpH. The experiments are analogous to those shown in Fig. 8 expect that valinomycin and CCP were not present.

ΔpH and the transport kinetics of Ca^{2+} ionophores. By using the present system, the uncertainty in the indicated values of internal pH seem to be on the order of ±0.05 U (Figs. 1 and 2, Table 2), with errors in the estimation of the internal $Cs^+(K^+)$ concentration and resulting errors in the estimation of the BCECF pK_a probably accounting for most of this range (Fig. 3). Because the pK_a of BCECF is strongly dependent on ionic strength (Fig. 1), the effect of Ca^{2+} transport and the resulting effect on the free-complexed state of internal Quin-2 on internal ionic strength must also be considered as a potential source of error. When there are no provisions for minimizing ΔpH, all three Ca^{2+} ionophores transport Ca^{2+} in strict exchange for $2H^+$ under the conditions used here (Erdahl et al., 1994). In that case, the loss of contributing negatively charged groups resulting from Ca^{2+} binding to Quin-2 will be largely balanced by further ionization of internal Hepes, resulting in no significant change in internal ionic strength. When valinomycin plus CCP are present to reduce ΔpH, the combined action of these agents plus the Ca^{2+} ionophore will produce a net exchange of Ca^{2+} for $2Cs^+$. In that case, the loss of internal Cs^+ plus the reduction in contributing negatively charged groups resulting from Ca^{2+} binding to Quin-2 will reduce the internal content of ionic species, potentially reducing ionic strength. However, because internal Cs^+ contributes

to internal osmotic pressure, there should be a contraction of the internal volume resulting in maintenance of ionic strength at near its initial value. Thus, mismatching of the internal and external K^+ concentrations during calibration of BCECF remains as the most probable source of error in the present estimates of internal pH. Similar uncertainties probably exist when BCECF is used in biological systems because the effects of internal and external K^+ concentrations on the apparent value of pK_a are not normally taken into account when calibrating the entrapped indicator. The accuracy of the present internal pH measurements are adequate for our purposes because the magnitudes of the ΔpH values considered here are severalfold larger than the range of uncertainty.

Origin of ΔpH effects on Ca^{2+} transport kinetics

A ΔpH in the range of 0.4–0.6 U clearly has significant effects on the transport properties of Ca^{2+} ionophores (Figs. 4–6, Table 3). It is important to emphasize that these effects, which are identified here by collapsing ΔpH and by observing the accompanying changes in rate and extent of transport, truly arise from the change in pH conditions produced by valinomycin plus CCP. An alternate interpretation might be that valinomycin plus CCP collapses a membrane potential that had formed during preceding electrogenic Ca^{2+} transport and that loss of this membrane potential caused the changes in Ca^{2+} transport kinetics. This interpretation is not viable because no membrane potential is detected when these ionophores transport Ca^{2+} in the absence of valinomycin plus CCP (Erdahl et al., 1994, and data not shown), because nigercin can be used in place of valinomycin plus CCP, and because neither valinomycin nor CCP used alone can substitute for both agents used in combination (see Results). It is also important to emphasize that the consequences of collapsing a ΔpH cannot be ascribed to the changes in absolute pH within the vesicle lumen and are thus due to changes in ΔpH per se. This is apparent when Figs. 4–6 are compared with Fig. 7, which shows that small changes in absolute pH produce changes in the rate and extent of Ca^{2+} transport that are of opposite sign to those produced by a ΔpH of the same magnitude.

It is possible to explain the effects of a ΔpH on the transport kinetics of Ca^{2+} ionophores when it is recalled that in the uncomplexed form, these compounds are weak acids and are membrane permeable when not ionized. Accordingly, they will distribute across a membrane in accordance with ΔpH, as do acetate ions, ammonia, and free fatty acids, for example. This tendency to equilibrate transmembrane distribution with ΔpH is illustrated in Fig. 10 *A*, which emphasizes that the equilibration between transmembrane ionophore distribution and ΔpH can proceed independently of the reactions involved in Ca^{2+} transport per se. However, the distribution that is attained will markedly affect initial rate kinetics, as illustrated in Fig. 10 *B* (see also Vestergaard-Bogind and Stampe, 1984). Were the ΔpH equal to 0.4 U for example, the ratio A_{in}/A_{out} would be 2.5 if this ratio and ΔpH were fully equilibrated. The initial rate of Ca^{2+} uptake is a function of ionophore availability at outer membrane interface where the transporting species is formed. A ΔpH, inside basic, would then be expected to reduce the initial rate of Ca^{2+} uptake compared with the rate obtained in the absence of a ΔpH because it would reduce the availability of ionophore at the outer membrane interface. A reduced rate is in fact observed (Figs. 4–6, Table 3), and we can attribute this effect of ΔpH on initial rate kinetics to an unequal ionophore distribution between the two sides of the membrane.

The effect of ΔpH on transmembrane ionophore distribution can also explain, from a kinetic perspective, why the collapse of ΔpH increases the extent of Ca^{2+} transport into the vesicles. As a maximal extent of Ca^{2+} transport is approached, the rates of transport into and out of the vesicles are approaching the same value (Fig. 10 *C*). Similar to the situation described for initial rates, these opposing rates are given by the transmembrane diffusion constant of the transporting species multiplied by the concentration of that species at the outer and inner membrane interfaces, respectively. Because the interfacial concentration of the transporting species will depend on the concentration of free ionophore at the interface (as well as the ionization state and the local Ca^{2+} concentration), a ΔpH-driven accumulation of ionophore on one side of the membrane will favor the rate of transport initiating on that side, compared with the opposing rate. When the ΔpH orientation is inside basic, the $rate_{out}$ is favored over the $rate_{in}$ when the concentrations of free Ca^{2+} on both sides of the membrane are equal. For these rates to become equal, as must be the case when a maximal extent of Ca^{2+} transport has been attained, the concentration of free Ca^{2+} inside would have to be lower than that outside (Fig. 10 *C*). These considerations seem to explain why the uptake reaction fails to readily saturate internal Quin-2 because they predict that collapsing ΔpH would allow uptake to proceed toward completion and that is what is observed (Figs. 4–6, Table 3). Through extension of the above arguments, it becomes clear why it should not be assumed that Ca^{2+} ionophores will readily equilibrate ΔpCa with ΔpH when ΔpH is not equal to zero. The rate of transport from the basic side of the membrane could closely approach the rate from the acidic side well before thermodynamic equilibrium between the two gradients is attained because of a higher steady-state level of ionophore on the basic side.

Apparently there is a second factor involved in limiting the equilibration of ΔpCa and ΔpH as shown by Figs. 8 and 11. The data in Fig. 8 were obtained in the presence of valinomycin plus CCP so that a minimal or no ΔpH would be present throughout (this was verified in parallel experiments (not shown) that monitored internal pH by BCECF flourescence). Under these conditions, full equilibration between the two gradients would produce a $[Ca^{2+}]_{in}/[Ca^{2}]_{out}$ ratio of 1. Such ratios were computed from the data in Fig. 8 and are shown in Fig. 11. They are far above 1 in all cases,

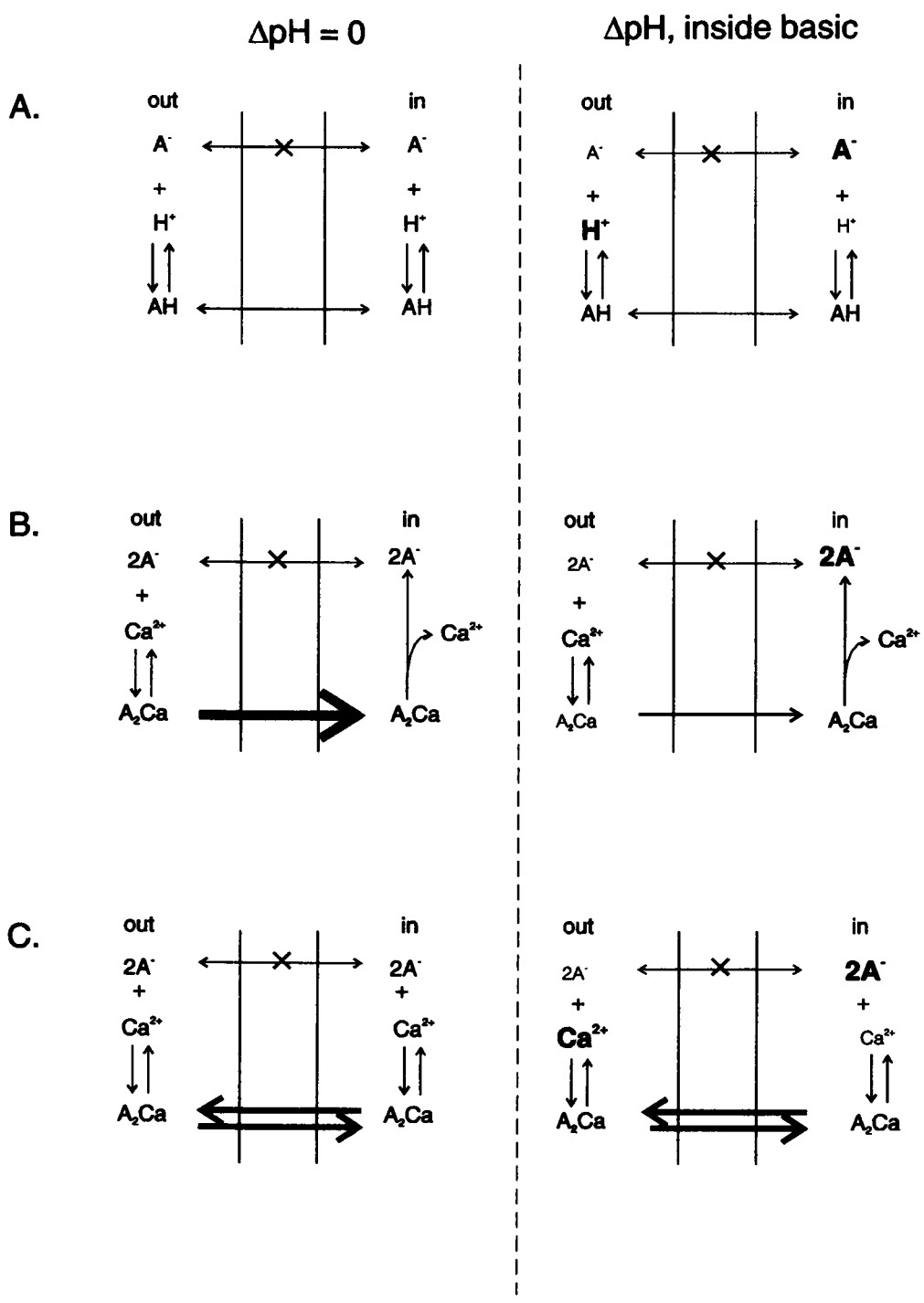

FIGURE 10 Illustration of relationships between ΔpH, transmembrane ionophore distribution, and the kinetics of Ca^{2+} transport. The pairs of vertical lines represent sections of the vesicle membrane with the internal (*in*) and external (*out*) volumes oriented as shown. The anionic forms of Ca^{2+} ionophores are membrane impermeable, as indicated by the X in each half of the three panels. Situations depicted to the left of the center line are expected when ΔpH = 0; those on the right show qualitatively how the situation would change if an inside basic ΔpH were present. The size and boldness of symbols reflect relative concentrations and relative rates. Thus in A, left side, all symbols are the same size, reflecting the absence of concentration gradients for H^+, HA, and A^-, which is expected when ΔpH = 0. The right side of A shows that in comparison, a ΔpH, inside basic, will raise the level of A^- inside and lower it outside. B illustrates the expected reduction in the initial rate of Ca^{2+} transport into the vesicles, which is expected in the presence of a ΔpH, and that the reduced rate is caused by a lowered concentration of A_2Ca (the transporting species) at the outer membrane interface. C illustrates how a ΔpH is expected to influence the relative free Ca^{2+} concentrations in the external and internal compartments, at the condition where opposing rates of transport into and out of the vesicles are equal (i.e., at the maximal extent of Ca^{2+} uptake). At ΔpH = 0, the two Ca^{2+} concentrations would be equal because the levels of A^- and A_2Ca would be the same on both sides of the membrane. In the presence of an inside basic ΔpH, equal opposing rates should occur when the Ca^{2+} concentration inside was lower than outside because of the reverse orientation of the A^- gradient and the requirement that the A_2Ca level be the same on both sides of the membrane.

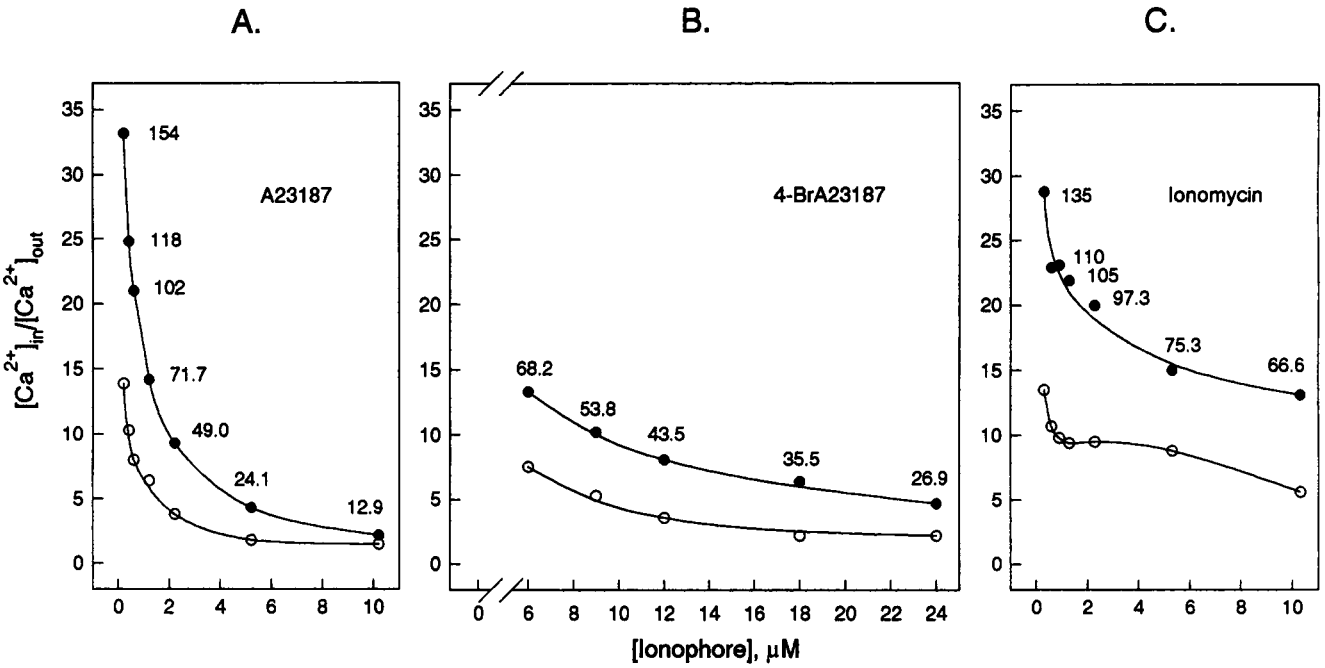

FIGURE 11 The effect of ionophore concentration on equilibration of transmembrane Ca^{2+} concentration gradients. Sections of the progress curves shown in Figs. 8 and 9, after the second addition of Ca^{2+} ionophore, were fit to Eq. 3 to estimate the maximum extent of Ca^{2+} release from the vesicles. The internal free Ca^{2+} concentration was then calculated for that extent of Ca^{2+} release from the internal Quin-2 concentration, the ratio of Quin-2:free/Quin-2:Ca^{2+} at that extent of release, and the dissociation constant of the Quin-2:Ca^{2+} complex. The latter value was obtained from the Fabiato program (Fabiato and Fabiato, 1979). This value is only slightly dependent on pH in the region above 7, and this small dependence was taken into account using the internal pH measurements, which were carried out in parallel with the experiments shown in Figs. 8 and 9 (data not shown). The external free Ca^{2+} concentrations were calculated from the total EDTA concentration, the fraction of Ca^{2+} not bound to Quin-2, and the dissociation constant of the EDTA:Ca^{2+} complex, which was taken to be 57 nM at the external pH value of 7.0 (Fabiato and Fabiato, 1979). The ratio of free Ca^{2+} concentrations (inside/outside) could then be calculated at the maximal extents of Ca^{2+} release, and these are the values plotted in the figure, as a function of ionophore concentration. A, B, and C were obtained with ionophores A23187, 4-BrA23187, and ionomycin, respectively. For all panels, (●), ΔpH absent (i.e., valinomycin plus CCP present); (○), ΔpH present (i.e., valinomycin plus CCP absent). The numbers associated with the individual points (●) are the calculated free Ca^{2+} concentrations within the vesicles at the maximal extents of Ca^{2+} release. The calculated external free Ca^{2+} concentrations varied from about 4.5 to ~6.0 nM across the range of internal free Ca^{2+} concentrations encountered during these experiments.

although they tend toward that value at high ionophore concentrations, particularly in the case of A23187. Two factors suggest that poor equilibration under these conditions is caused, at least in part, by limited formation of the transporting species at the inner membrane interface. The first is that equilibration is approached progressively as the ionophore concentration is increased (Fig. 11). This suggests that complex formation becomes limiting because increasing the ionophore concentration will drive formation of the transporting species by mass action, although this effect should be manifest on both sides of the membrane. The importance of complex formation on the inner side of the membrane is indicated by the fact that an inside basic ΔpH shifts the $[Ca^{2+}]_{in}/[Ca^{2+}]_{out}$ ratio to lower values across the entire range of ionophore concentration examined (Figs. 9 and 11). A ΔpH with this orientation would shift ionophore distribution toward the inner membrane surface favoring complex formation on that side, as described above. Therefore, it is complex formation at the inner membrane interface that seems to be retarding equilibration of the Ca^{2+} gradient when ΔpH = 0.

What is not clear at present is why complex formation on the inner surface becomes limiting. One possibility is that free ionophore molecules associate with Quin-2:Ca^{2+} or EDTA:Ca^{2+} or both to form mixed complexes that render the ionophores less available for Ca^{2+} transport. A second possibility is that unrecognized interactions occur between the ionophores and Cs^+, or components of the pH buffer system, and that these interactions compete for association with Ca^{2+}. It might also be argued that neither Eq. 2 nor Eq. 3 adequately represents the transport process under the conditions of Figs. 8 and 9 and that the Ca^{2+} concentration gradients would reach the expected values if the experiments were extended to very long times. Although it is true that all gradients would reach equilibrium given enough time, we have extended experiments like those in Figs. 8 and 9 to periods of 1 h and have seen good agreement between the projected and observed extents of Ca^{2+} release (data not shown). Regardless of why these ionophores do not readily equilibrate ΔpCa and ΔpH, it should be noted that this result points to some possible problems with how Ca^{2+} ionophores are used to investigate biological systems. For example, under the conditions of Figs. 8 and 9, the free Ca^{2+} concentrations that exist in the vesicles bracket the resting cytosolic free Ca^{2+} concentration in a typical cell (e.g., 50–100 nM). In addition, the time frames allowed for

Ca^{2+} release in Figs. 8 and 9 are long compared with those sometimes used in studies of biological systems, and the ionophore concentrations extend to higher values than are commonly used. Thus it seems uncertain whether ionophores plus an external chelator can be relied upon to maintain cytosolic Ca^{2+} levels below the range in which they influence cell signaling mechanisms, as is sometimes assumed. Other practices that seem questionable on the basis of the present findings include using Ca^{2+} ionophores in the absence or presence of a ΔpH to calibrate fluorescent Ca^{2+} indicators trapped within cells, and application of the so-called null point titration technique to estimate the free concentration of a divalent cation within cells or subcellular structures.

Do Ca^{2+} ionophores transport electrogenically?

Although additional work is required to determine to what extent the possible problems pointed out above actually occur when Ca^{2+} ionophores are used in biological systems, it seems that these compounds are unlikely to produce significant biological actions by altering membrane potentials through electrogenic Ca^{2+} transport. This is because the data that have been taken to support the existence of electrogenic modes can be explained as ΔpH effects on the rate and extent of Ca^{2+} transport. In the case of our own data, we estimated that as many as 1 in 10 transport events could be electrogenic, but only when a large membrane potential was imposed across the membrane. This estimate was on the basis of the initial rate increases of a few percent and similar increases in the extents of transport, which were produced by an imposed potential (Erdahl et al., 1994). Very small changes in ΔpH produced by movement of H^+ and/or other medium components down electrochemical gradients would seem to be adequate to explain those previous findings when the data in Figs. 4–6 and Table 3 are considered. (The changes in internal pH that would be required to explain our previous findings are within the error range of the BCECF method used here. However, during long time-frame experiments, we have found that in the presence of a 150 mV imposed potential (inside negative), the internal pH becomes more acidic at a rate of ~0.1 units/10 min (data not shown)). The findings of Fascilato and Pozzan (1989), which were obtained with intact cells and multilamellar vesicles, may have been seen because small changes in ΔpH occurred when their systems were permeabilized with gramicidin rather than because the ionophores transport Ca^{2+} electrogenically, as they proposed. In the case of their data obtained with cells, it has also been shown that the opening of endogenous Ca^{2+}-regulated Ca^{2+} channels in the plasma membrane can explain the apparent electrogenic transport activity of ionomycin (Mason and Grinstein, 1993).

Thus at present there are no data that clearly indicate that these ionophores transport Ca^{2+} electrogenically through a carrier type of mechanism. At the same time, there are several lines of evidence which indicate that they substantially lack that activity. Notable among these are the inability of A23187 or ionomycin to allow Ca^{2+} uptake into ruthenium red-inhibited mitochondria (Reed and Lardy, 1972; Kauffman et al., 1980) and the failure of these compounds to produce measurable charge movements across planar bilayer membranes, as noted in the Introduction. These are strong arguments against an electrogenic activity because a membrane potential is present in both systems and the orientation of the potential would drive transport via the species ACa^+, $4\text{-}BrACa^+$, and $IHCa^+$, if it could occur. These are the species that were thought to provide an electrogenic transport mode for ionophores A23187, 4-BrA23187, and ionomycin, respectively (e.g., Chapman et al., 1990b; Fasolato and Pozzan, 1989). Apparently, in these species the calcium ion is not sufficiently shielded from solvent interactions, and/or the net positive charge is not sufficiently delocalized to allow for ready permeation of a phospholipid membrane.

The above analysis is predicated on the assumption that electrogenic Ca^{2+} transport would occur through a carrier-mediated mechanism. Recent work by Easwaran and coworkers has raised the possibility that A23187 can form ion-conducting channels, particularly during longer time-frame experiments (Balasubramanian et al., 1992; Jyothi et al., 1994). Although not a carrier-mediated mechanism, the movement of Ca^{2+} through channels would also be electrogenic. The relationship of their findings to those reported here will be described in a subsequent publication (Thomas, Pfeiffer, and Taylor, manuscript submitted).

This research was supported by United States Public Health Service Grant HL49181 from the National Institutes of Health, National Heart, Lung and Blood Institute.

REFERENCES

Balasubramanian, S. V., S. K. Sikdar, and K. R. K. Easwaran. 1992. Bilayers containing calcium ionophore A23187 form channels. *Biochem. Biophys. Res. Commun.* 189:1038–1042.

Bartlett, G. R. 1959. Phosphorus assay in column chromatography. *J. Biol. Chem.* 234:466–468.

Chapman, C. J., A. K. Puri, R. W. Taylor, and D. R. Pfeiffer. 1987. Equilibria between ionophore A23187 and divalent cations: stability of 1:1 complexes in solutions of 80% methanol/water. *Biochemistry.* 26: 5009–5018.

Chapman, C. J., W. L. Erdahl, R. W. Taylor, and D. R. Pfeiffer. 1990a. Factors affecting solute entrapment in phospholipid vesicles prepared by the freeze-thaw extrusion method: a possible general method for improving the efficiency of entrapment. *Chem. Phys. Lipids.* 55:73–84.

Chapman, C. J., A. K. Puri, R. W. Taylor, and D. R. Pfeiffer. 1990b. General features in the stoichiometry and stability of ionophore A23187-cation complexes in homogeneous solution. *Arch. Biochem. Biophys.* 281:44–57.

Chapman, C. J., W. L. Erdahl, R. W. Taylor, and D. R. Pfeiffer. 1991. Effects of solute concentration on the entrapment of solutes in phospholipid vesicles prepared by freeze-thaw extrusion. *Chem. Phys. Lipids.* 60:201–208.

Erdahl, W. E., C. J. Chapman, R. W. Taylor, and D. R. Pfeiffer. 1994. Ca^{2+} transport properties of ionophores A23187, ionomycin, and 4-BrA23187 in a well defined model system. *Biophys. J.* 66:1678–1693.

Fabiato, A., and F. Fabiato. 1979. Calculator programs for computing the composition of the solutions containing multiple metals and ligands used for experiments in skinned muscle cells. *J. Physiol. (Paris).* 75:463–505.

Fasolato, C., and T. Pozzan. 1989. Effect of membrane potential on divalent cation transport catalyzed by the "electroneutral" ionophores A23187 and ionomycin. *J. Biol. Chem.* 264:19630–19636.

Fry, D. W., J. C. White, and D. Goldman. 1978. Rapid separation of low molecular weight solutes from liposomes without dilution. *Anal. Biochem.* 90:809–815.

Hope, M. J., M. B. Bally, G. Webb, and P. R. Cullis. 1985. Production of large unilamellar vesicles by a rapid extrusion procedure. Characterization of size distribution, trapped volume and ability to maintain a membrane potential. *Biochim. Biophys. Acta.* 812:55–65.

Jyothi, G., A. Surolia, and K. R. K. Easwaran. 1994. A23187-Channel behaviour: fluorescence study. *J. Biosci.* 19:277–282.

Kafka, M. S., and R. W. Holz. 1976. Ionophores X537A and A23187. Effects on the permeability of lipid bimolecular membranes to dopamine and calcium. *Biochim. Biophys. Acta.* 426:31–37.

Kamo, N., M. Muratsugu, R. Hongoh, and Y. Kobatake. 1979. Membrane potential of mitochondria measured with an electrode sensitive to tetraphenylphosphonium and relationship between proton electrochemical potential and phosphorylation potential in steady state. *J. Membr. Biol.* 49:105–121.

Kauffman, R. F., R. W. Taylor, and D. R. Pfeiffer. 1980. Cation transport and specificity of ionomycin: comparison with ionophore A23187 in rat liver mitochondria. *J. Biol. Chem.* 255:2735–2739.

Kauffman, R. F., R. W. Taylor, and D. R. Pfeiffer. 1982. Acid-base properties of ionophore A23187 in methanol/water solutions and bound to unilamellar vesicles of dimyristoylphosphatidylcholine. *Biochemistry.* 21:2426–2435.

Kauffman, R. F., C. J. Chapman, and D. R. Pfeiffer. 1983. Location and dynamics of ionophore A23187 bound to unilamellar vesicles of dimyristoylphosphatidylcholine. *Biochemistry.* 22:3985–3992.

Mason, M. J., and S. Grinstein. 1993. Ionomycin activates electrogenic Ca^{2+} influx in rat thymic lymphocytes. *Biochem. J.* 296:33–39.

Mayer, L. D., M. J. Hope, and P. R. Cullis. 1986. Vesicles of variable sizes produced by a rapid extrusion procedure. *Biochim. Biophys. Acta.* 858: 161–168.

Moronne, M. M., and J. A. Cohen. 1982. Electrical measurement of electroneutral fluxes of divalent cations through charged planar phospholipid membranes. *Biochim. Biophys. Acta.* 688:793–797.

O'Shea, P. S., G. Petrone, R. P. Casey, and A. Azzi. 1984. The current-voltage relationships of liposomes and mitochondria. *Biochem. J.* 219: 719–726.

Pfeiffer, D. R., R. W. Taylor, and H. A. Lardy. 1978. Ionophore A23187: cation binding and transport properties. *Ann. N. Y. Acad. Sci.* 307: 402–423.

Reed, P. W., and H. A. Lardy. 1972. A23187: a divalent cation ionophore. *J. Biol. Chem.* 247:6970–6977.

Rink, T. J., R. Y. Tsien, and T. Pozzan. 1982. Cytoplasmic pH and free Mg^{2+} in lymphocytes. *J. Cell Biol.* 95:189–196.

Sankaram, M. B., B. P. Shastri, and K. R. K. Easwaran. 1987. Interaction of carrier ionophores with phospholipid vesicles. *Biochemistry.* 26: 4936–4941.

Smith, G. L., and D. J. Miller. 1985. Potentiometric measurements of stoichiometric and apparent affinity constants of EGTA for protons and divalent ions including calcium.. *Biochim. Biophys. Acta.* 839:287–299.

Stiles, M. K., M. E. Craig, S. L. N. Gunnell, D. R. Pfeiffer, and R. W. Taylor. 1991. The formation constants of ionomycin with divalent cations in 80% methanol/water. *J. Biol. Chem.* 266:8336–8342.

Taylor, R. W., R. F. Kauffman, and D. R. Pfeiffer. 1982. Cation complexation and transport by carboxylic acid ionophores. *In* Polyether Antibiotics. Naturally Occurring Acid Ionophores, Vol. I, Chapter 4. J. W. Westley, editor. Marcel Dekker, New York. 103–184.

Thomas, J. A., R. N. Buchsbaum, A. Zimniak, and E. Racker. 1979. Intracellular pH measurements in *Ehrlich Ascites* tumor cells utilizing spectroscopic probes generated in situ. *Biochemistry.* 18:2210–2218.

Tsien, R. Y. 1980. New calcium indicators and buffers with high selectivity against magnesium and protons: design, synthesis, and properties of prototype structures. *Biochemistry.* 19:2396–2404.

Vega, C. A., and R. G. Bates. 1976. Buffers for the physiological pH range: thermodynamic constants of four substituted aminoethanesulfonic acids from 5 to 50 degrees C. *Anal. Chem.* 48:1293–1296.

Vestergaard-Bogind, B., and P. Stampe. 1984. *Trans* to *Cis* proton concentration gradients accelerate ionophore A23187-mediated net fluxes of Ca^{2+} across the human red cell membrane. *Biochim. Biophys. Acta.* 775:328–340.

Wulf, J., and W. G. Pohl. 1977. Calcium ion-flux across phosphatidylcholine membranes mediated by ionophore A23187. *Biochim. Biophys. Acta.* 465:471–485.

Yuchi, A., A. Tanaka, M. Hirai, T. Yasui, H. Wada, and G. Nakagawa. 1993. Complexation equilibria and fluorescent properties of chelating reagents derived from ethylene, glycol vis (β-aminoethylether)-*N,N,N'* - tetraacetic acid. *Bull. Chem. Soc. Jpn.* 66:377–3381.